Hadronic Signature of Quark-Gluon Plasma*

Johann Rafelski[a†] and Jean Letessier[b]

[a]Department of Physics, University of Arizona, Tucson, AZ 85721
and
[b]Laboratoire de Physique Théorique et Hautes Energies[‡]
Université Paris 7, 2 place Jussieu, F–75251 Cedex 05.

September 2002

Abstract

We discuss how hadronic particle production can help to identify the new form of matter created at RHIC and SPS. We use statistical hadronization approach and allow for chemical non-equilibrium. Strangeness production is shown to lead to near full saturation of the deconfined quark–gluon phase space as is seen in terms of highly over saturated final state hadron phase space.

1 Statistical Hadronization

Statistical Fermi-Pomeranchuk models have been used extensively to study particle yields and spectra since 1950 [1, 2]. This approach was proposed as a qualitative description of the gross features of particle production seen in cosmic ray events. Since, considerable refinement of the model has occurred which allows to use particle yields to study the physical properties of particle source. This is done determining the chemical fireball properties at the time of soft hadron production [3].

The particle yields are controlled by fireball temperature T and fugacities Υ_i of particle type 'i'. These comprise two types of chemical statistical factors, as noted in the example for the nucleon, and the antinucleon:

$$\Upsilon_N = \gamma_N e^{\mu_{\rm B}/T} \equiv e^{\sigma_N/T}, \quad \Upsilon_{\overline{N}} = \gamma_N e^{-\mu_{\rm B}/T} \equiv e^{\sigma_{\overline{N}}/T}, \tag{1}$$

*In proceedings of *Quark Confinement and the Hadron Spectrum (Confinement V)* Editors: N. Brambilla, G.M. Prosperi; pp.42-51 (World Scientific 2003)

†Supported by grant DE-FG03-95ER40937 from the U.S. Department of Energy.

‡LPTHE, Univ. Paris 6 et 7 is: Unité mixte de Recherche du CNRS, UMR7589.

$$\sigma_N \equiv \mu_{\rm B} + T\ln\gamma_N, \quad \sigma_{\overline{N}} \equiv -\mu_{\rm B} + T\ln\gamma_N.$$

There is an obvious difference between the two chemical factors in Eq. (1): the number of nucleon-antinucleon pairs is associated with the value of γ_N but not with $\mu_{\rm B}$. This can be seen looking at the first law of thermodynamics, in this context written as:

$$\begin{aligned} dE &= -P\,dV + T\,dS + \sigma_N\,dN + \sigma_{\overline{N}}\,d\overline{N}, \\ &= -P\,dV + T\,dS + \mu_{\rm B}(dN - d\overline{N}) + T\ln\gamma_N(dN + d\overline{N}). \end{aligned} \tag{2}$$

We see that $\mu_{\rm B}$ is the energy required to change the baryon number, $b \equiv N - \overline{N}$, by one unit, while the number of nucleon-antinucleon pairs, $2N_{\rm pair} \equiv N + \overline{N}$, is related to γ_N. For $\gamma_N \to 1$, the last term vanishes, at this point small fluctuation in number of nucleon pairs does not influence the energy of the system, we have reached the absolute baryochemical equilibrium.

It is convenient to follow the quark flavor even in the study of hadron yields, since this allows to keep the same notation across the phase boundary of quark matter and hadronic gas matter. We use:

$$\lambda_u = e^{\mu_u/T},\ \lambda_d = e^{\mu_d/T},\ \lambda_s = e^{\mu_s/T},\ \mu_q = \frac{1}{2}(\mu_u + \mu_d),\ \lambda_q^2 = \lambda_u\lambda_d. \tag{3}$$

When the light flavors u, d remain indistinguishable we introduce λ_q.

The relationship of baryochemical potential $\mu_{\rm B}$ and of strangeness chemical $\mu_{\rm S}$ to quark chemical potential is:

$$\mu_{\rm B} = 3\mu_q, \quad \lambda_{\rm B} = \lambda_q^3, \qquad \lambda_{\rm S} = \frac{\lambda_q}{\lambda_s}, \quad \mu_{\rm S} = \frac{1}{3}\mu_{\rm B} - \mu_s. \tag{4}$$

These relations arise considering that three quarks make a baryon, and remembering that strange quarks carry *negative* strangeness and one third of baryon number.

Near to chemical equilibrium, we use three non-equilibrium parameters, γ_s, and γ_u, γ_d or equivalently just two parameters introducing, $\gamma_q = \sqrt{\gamma_u\gamma_d}$. In quark matter, these coefficients express the approach to the expected chemical equilibrium yield by the quark abundances. In a coalescence hadronization process, gluons fragment into quark pairs and the net yields of quarks and antiquarks of all flavors is redistributed among all individual hadrons. Hence even if there were no change of the quark pair number in hadronization, the values of $\gamma_u, \gamma_d, \gamma_s$ in hadron gas and quark matter must differ. Moreover, the phase spaces have different size, and it is impossible in the rapidly evolving fireballs to re-equilibrate several quark flavors. Thus, we have to distinguish:

$$\gamma_u^{\rm QGP}, \gamma_d^{\rm QGP}, \gamma_s^{\rm QGP}, \quad \text{from} \quad \gamma_u^{\rm HG}, \gamma_d^{\rm HG}, \gamma_s^{\rm HG}.$$

It is best to see how this works looking at typical examples:
a) baryons: protons $p(uud)$, antiprotons $\bar{p}(\bar{u}\bar{u}\bar{d})$, $\Lambda(uds)$, etc:

$$\Upsilon_p = \gamma_u^2\gamma_d\, e^{2\mu_u+\mu_d},\ \Upsilon_{\bar{p}} = \gamma_u^2\gamma_d\, e^{-2\mu_u-\mu_d},\ \Upsilon_\Lambda = \gamma_u\gamma_d\gamma_s\, e^{\mu_u+\mu_d+\mu_s}. \tag{5}$$

b) mesons: $\pi^+(u\bar{d})$, $\pi^-(\bar{u}d)$, $K^-(\bar{u}s)$, etc:

$$\Upsilon_{\pi^+} = \gamma_u\gamma_d\, e^{\mu_u-\mu_d}, \quad \Upsilon_{\pi^-} = \gamma_u\gamma_d\, e^{-\mu_u+\mu_d}, \quad \Upsilon_{K^-} = \gamma_u\gamma_s\, e^{-\mu_u+\mu_s}. \tag{6}$$

Note that in the products of particle $\Upsilon_{\rm P}$ and antiparticle $\Upsilon_{\rm A}$ fugacities the chemical potentials μ_i always cancel $\Upsilon_{\rm P}\Upsilon_{\rm A} = f(\gamma_i)$.

In the statistical hadronization approach, we have the same value of Υ for all hadrons with the same valance quark content. For example $\Upsilon_p = \Upsilon_{\Delta^+}$. Thus, we assume tacitly that the relative population of heavier resonances is in chemical equilibrium with the lighter states. This means that statistical hadronization solely focuses on the valance quark and antiquark distribution and does not allow for the possibility that heavier resonances may simply not be populated. This method, thus, is most suitable for a hadronizing quark matter fireball, and may miss important features of a hadron fireball which never entered the deconfined phase.

Using of fugacities which follow the yield of quarks, $\lambda_i,\ i = u, d, s$, particle yields can be easily checked, and thus errors and omissions in a rather complex large particle 'zoo' minimized. Consider, as an example, the ratio of a baryon and antibaryon with strangeness and for reasons which will become obvious in a moment, we choose to look at the ratio $\overline{\Xi^-}(\bar{d}\bar{s}\bar{s})/\Xi^-(dss)$. Given the quark content and ignoring (at RHIC very small) isospin asymmetry, we find:

$$\frac{\overline{\Xi^-}}{\Xi^-} = \frac{\lambda_s^{-2}\lambda_q^{-1}}{\lambda_s^2\lambda_q} = \lambda_s^{-4}\lambda_q^{-2} = e^{-4\,\mu_s/T}e^{-2\mu_q/T} = e^{4\,\mu_{\rm S}/T}e^{-2\mu_{\rm B}/T}. \tag{7}$$

Since all Ξ resonances which contribute to this ratio are symmetric for particles and antiparticles, and possible weak interaction feed from $\overline{\Omega}(\bar{s}\bar{s}\bar{s})$, and respectively $\Omega(sss)$, are small, these expressions are actually nearly exact. Thus, we have inverted the relation and expressed $\mu_{\rm S}$ in terms of $\mu_{\rm B}$ and the cascade ratio. This allows the reader to check if results on $\mu_{\rm B,\mu_S}$ presented elsewhere are correct.

As can be seen in Eq. (7), when we compare in a ratio the particle with its antiparticle we measure chemical potentials. In order to determine the chemical non-equilibrium parameters without the burden of fixing the chemical potential, ratio of *products* of yields of particles and antiparticles must be considered, in which the chemical potentials μ_i cancel. As example consider the three ratios controlled by the two parameters T and γ_s/γ_q:

$$\sqrt{\frac{\Xi\overline{\Xi}}{\Lambda\overline{\Lambda}}} \propto \frac{\gamma_s}{\gamma_q}\, e^{-\frac{m_\Xi - m_Y}{T}};\ \sqrt{\frac{\Lambda\overline{\Lambda}}{p\bar{p}}} \propto \frac{\gamma_s}{\gamma_q}\, e^{-\frac{m_\Lambda - m_N}{T}};\ \sqrt{\frac{K\overline{K}}{\pi\overline{\pi}}} \propto \frac{\gamma_s}{\gamma_q}\, e^{-\frac{m_K - m_\pi}{T}}. \tag{8}$$

Both γ_s and γ_q differ generally from unity, though often only $\gamma_s \neq 1$ is considered, see section 2. $\gamma_q > 1$ helps to transform the entropy rich QGP into hadron gas. We see this best considering the properties of the pion gas as function of γ_q, and in particular, the entropy, with:

$$S_\pi = \int \frac{d^3p\, d^3x}{(2\pi\hbar)^3}\, \left[(1+f_\pi)\ln(1+f_\pi) - f_\pi \ln f_\pi\right], \quad f_\pi = \frac{1}{\gamma_q^{-2}e^{\frac{E_\pi}{T}} - 1}. \tag{9}$$

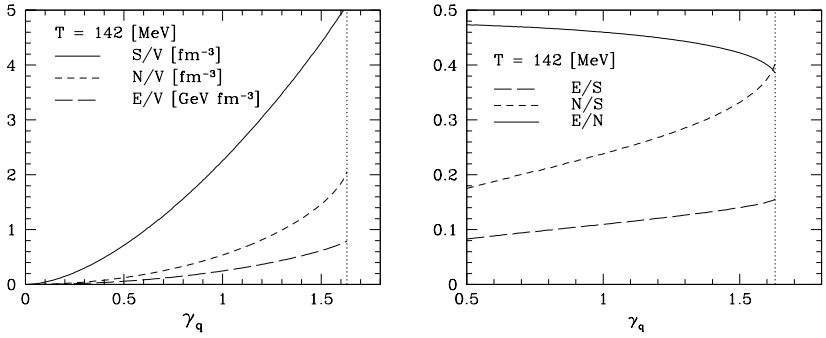

Figure 1: Pion gas properties as function γ_q.

Here, $E_\pi = \sqrt{m_\pi^2 + p^2}$. We see, in figure 1, that the entropy density is rising rapidly and it nearly doubles with γ_q increasing from the equilibrium value $\gamma_q = 1$ towards condensation point $\gamma_q^2 = e^{m_\pi/T}$. This high entropy content of the over saturated pion gas allows the sudden hadronization of QGP without extensive mixed phase. A striking feature of the experimental data analysis we show in last section is natural tendency towards the value $\gamma_q^2 = e^{m_\pi/T}$, which maximizes the entropy density in pion gas.

2 Kinetic Production of Strangeness

Among hadronic observables strangeness stands out. The production processes involving quark and the dominant gluon degrees of freedom in QGP were studied in the early eighties, for the quark process [4] and for the gluon process [5]. The lowest order flavor production cross sections are [6],

$$\sigma_{\mathrm{q\bar{q}}\to\mathrm{f\bar{f}}}(s) = \frac{8\pi\alpha_\mathrm{s}^2}{27s}\left(1+\frac{2m_\mathrm{f}^2}{s}\right)w(s), \quad w(s) = \sqrt{1-\frac{4m_\mathrm{f}^2}{s}}, \tag{10}$$

$$\sigma_{\mathrm{gg}\to\mathrm{f\bar{f}}}(s) = \frac{\pi\alpha_\mathrm{s}^2}{3s}\left[\left(1+\frac{4m_\mathrm{f}^2}{s}+\frac{m_\mathrm{f}^4}{s^2}\right)\ln\left(\frac{1+w(s)}{1-w(s)}\right)-\left(\frac{7}{4}+\frac{31m_\mathrm{f}^2}{4s}\right)w(s)\right]. \tag{11}$$

The contemporary results of strangeness production agree with the early results [5]. We see in Fig. 2 the time constants for chemical relaxation τ_s evaluated with $m_\mathrm{s}(1\mathrm{GeV}) = 200$ MeV. The range of the assumed 20% uncertainty in $m_\mathrm{s}(M_\mathrm{Z})$ is indicated by the hatched areas. The initial predictions obtained 20 years ago [5] are shown here at fixed values $\alpha_\mathrm{s} = 0.6$ for $m_\mathrm{s} = 200$ MeV (see thick dotted line in Fig. 2). The strange quark mass could be considerably smaller, as suggested by lattice studies of hadron properties, and the thin dotted line shows the relaxation time when the strange quark mass is reduced by a factor 5/9.

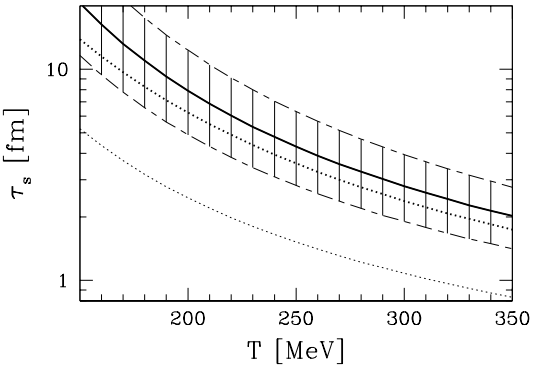

Figure 2: The QGP chemical relaxation time for strangeness $\tau_{\rm s}$, for $\alpha_{\rm s}(M_{\rm Z}) = 0.118$ with $m_{\rm s}(M_{\rm Z}) = 90$ MeV and $\rho_{\rm s}^{\infty}(m_{\rm s} \simeq 200\,{\rm MeV})$ (thick line). Hatched areas show the effect of the variation mass of the strange quark by 20%. The fat-dotted shows comparison results for fixed $\alpha_{\rm s} = 0.6$ and $m_{\rm s} = 200\,{\rm MeV}$. The thin-dotted line shows the result for $m_{\rm s}(M_{\rm Z}) = 50$ MeV.

Using strangeness relaxation time seen in Fig. 2, the time evolution of the strange quark flavor in rapidly evolving QGP can be fixed. For this we must model the time dependence of the temperature. For a purely longitudinal expansion, the local entropy density scales according to $S \propto T^3 \propto 1/\tau$. The transverse flow of matter accelerates the drop in entropy density. To model this behavior without too great a numerical effort, considering the other uncertainties, the following temporal-evolution function of the temperature is considered [7]:

$$T(\tau) = T_0 \left(\frac{1}{(1 + 2\tau c/d)(1 + \tau v_\perp / R_\perp)^2} \right)^{1/3}. \tag{12}$$

Considering various values of T_0, the temperature at which the gluon equilibrium is reached, the longitudinal dimension is scaled according to:

$$d(T_0) = (0.5\,{\rm GeV}/T_0)^3 \times 1.5\,{\rm fm}. \tag{13}$$

This adjustment of the initial volume V_0 assures that the different evolution cases refer to a fireball with a similar entropy content. The results are thus a study of one and the same collision system, and the curves reflect the uncertainty associated with unknown initial conditions of a fireball of quark–gluon plasma with in each case same entropy content.

The evolution with time in the plasma phase is followed up to the breakup of the QGP at a temperature $T_{\rm f}^{\rm RHIC} \simeq 150 \pm 5$ MeV. The numerical solution for $\gamma_{\rm s}$ is shown as a function both of time t, in Fig. 3(a), and of temperature T, in Fig. 3(b). This evolution is physically meaningful until it reaches the QGP breakup condition. Since the results for higher temperatures are also displayed, the reader who prefers a higher hadronization temperature can easily draw his own conclusions.

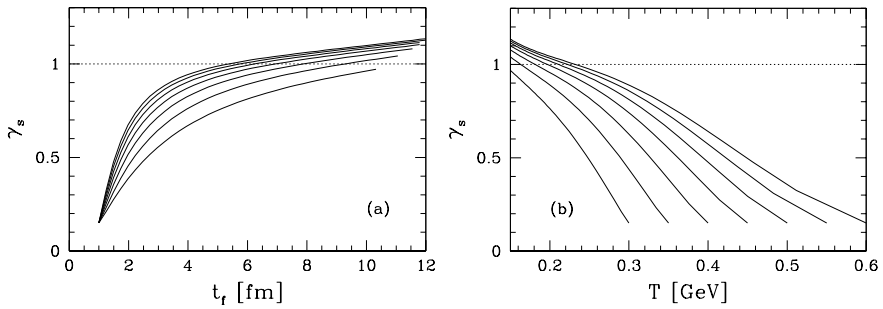

Figure 3: The evolution of QGP phase-space occupancy for strangeness $\gamma_{\rm s}$: (a) as a function of time and (b) as a function of temperature for $m_{\rm s}(1\,{\rm GeV}) = 200\,{\rm MeV}$; see text for details.

The results presented in Fig. 3 are typical for a RHIC energy collision system. At the top SPS energy range, the initial temperature is certainly less (by 10%–20%) than that in the RHIC-130 run, and the baryon number in the fireball is considerably greater; however, the latter difference matters little for production of strangeness, which is driven by gluons. A model similar to the above yields $\gamma_{\rm s}^{\rm QGP} \simeq 0.6$–$0.7$, the upper index reminds us that in this section the strangeness occupancy factor $\gamma_{\rm s}$ refers to the property of the deconfined phase. The final state $\gamma_s^{\rm HG}$ is about a factor 3 larger [3].

3 RHIC-130 Data Analysis

There are 6 chemical parameters, and the chemical freeze-out (hadronization) temperature. However, at RHIC, we need not distinguish the light flavors u, d and thus the number of statistical parameters is reduced by two. A further reduction is arrived at when we demand that strangeness balances anti-strangeness locally, and finally the requirement that when entropy rich quark–gluon plasma hadronizes, the yields of hadrons are maximizing the entropy content of hadrons, yields $\gamma_q^2 = e^{m_\pi/T}$. Thus, we are in fact needing just two chemical parameters which are usually λ_q and γ_s. Both at SPS [8] and at RHIC [9], there is good evidence for a single freeze-out to apply, in consistency with the sudden hadronization hypothesis. In other words, one single temperature allows to understand both yields and spectra of hadrons.

The computation of the particle yields for RHIC is much simpler than for SPS. For central rapidity, we have, at RHIC-130, approximate longitudinal scaling. Thus, we can act as if a series of fireballs at all rapidities was present. Then, we simply evaluate the full phase-space yields in order to obtain particle ratios.

First, we convince ourselves that the introduction of chemical non equilibrium in the study of hadron abundances is necessary. The ratios considered in Eq. (8) have only two parameters T and γ_s/γ_q. Thus, it is possible to present, in a two dimensional figure, how these three ratios behave, as is seen in figure 4 for the experimental data obtained

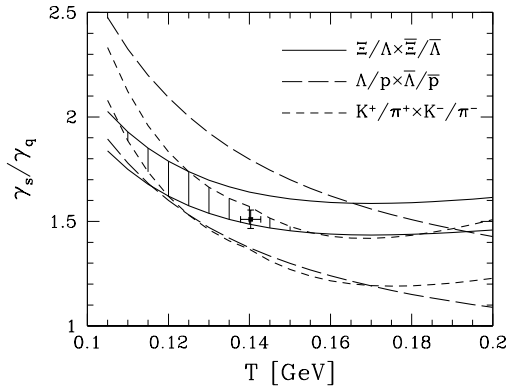

Figure 4: Ratios of products of particle and antiparticle abundances in the T-γ_s/γ_q plane. Ranges derived from data shown in table 1.

at RHIC-130 (see table 1 below). Dashed area shows the allowed parameter domain. The cross in the figure is the result of global data analysis, discusses below, where the ratio of baryons to mesons, not used here, fixes the temperature. While the kaon to pion ratio would tolerate within one standard deviation the chemical equilibrium, the baryon double ratios, and in particular the more strange cascades, are clearly demanding a value of $\gamma_s/\gamma_q > 1$.

To find this result we use the latest experimental results for the ratio of hyperons to nucleons ($\Lambda, \overline{\Lambda}$ uncorrected, nucleons $p, \bar{p}$ weak decay corrected) [10]. This result is nearly by a factor *two* different from the experimental data stated in [11], and this reference also does not consider $\Xi, \overline{\Xi}$ results other than their ratio, and is therefore consistent with the chemical equilibrium in the result of its analysis. It also is apparently correct as the test proposed below Eq. (7) shows. On the other hand this test fails other results [12]

A global fit [13] to the experimental data for RHIC-130 is given in table 1. We consider here 21 particle ratios. In some cases within the error other results from same and/or another collaboration are available, our selection is somewhat subjective, but does not influence in essential way the general conclusions which follow. In the three last columns, the results for both chemical equilibrium (last column) and non-equilibrium fits are seen.

Next to the fitted ratios, we show in parenthesis the contribution to the error (χ^2) for each entry. We consider statistical errors for the experimental results, since much of the systematic error should cancel in the particle ratios. However, we do not allow, when pion multiplicity is considered, for errors smaller than $\simeq 8\%$, which is our estimated error in the theoretical evaluation of the pion yield due to incomplete understanding of the high mass hadron resonances. Some of the experimental results are thus shown with a 'theoretical' error. When such an enlargement of the experimental error is introduced, a dagger as superscript appears in the experimental data second column in table 1.

Table 1: Central-rapidity hadron ratios at RHIC-$\sqrt{s_{\rm NN}}$ = 130 GeV. From top to bottom: experimental results, fitted chemical parameters, the physical properties of final state hadron phase-space, and the fitting error. Columns: ratio considered, data value with reference, two non-equilibrium fits, and in the last column, the chemical equilibrium fit. The superscript * indicates quantities fixed and not fitted. The superscript † indicates the error given is dominated by theoretical considerations. Subscripts Ξ, Λ mean that these values include weak cascading given in heading of table. In parenthesis, we show the contribution of the particular result to the total χ^2.

	Data	Ref.	$100\%\,\Xi \to Y$ $40\%\ \ Y \to N$	$40\%\,\Xi \to Y$ $40\%\,Y \to N$	$40\%\,\Xi \to Y$ $40\%\,Y \to N$
$\bar{p}/p$	0.71 ± 0.06	[10]	0.672(0.4)	0.677(0.3)	0.688(0.1)
$\overline{\Lambda}_\Xi/\Lambda_\Xi$	0.71 ± 0.04	[16]	0.750(1.0)	0.747(0.8)	0.757(1.4)
$\overline{\Xi}/\Xi$	0.83 ± 0.08	[14]	0.793(0.2)	0.803(0.1)	0.818(0.0)
$\mathrm{K}^-/\mathrm{K}^+$	0.87 ± 0.07	[15]	0.925(0.6)	0.924(0.6)	0.933(0.8)
$\mathrm{K}^-/\pi^\pm$	$0.15 \pm 0.02^\dagger$	[15]	0.156(0.1)	0.156(0.1)	0.150(0.0)
$\mathrm{K}^+/\pi^\pm$	$0.17 \pm 0.02^\dagger$	[15]	0.169(0.0)	0.170(0.0)	0.161(0.2)
Λ_Ξ/h^-	$0.059 \pm 0.004^\dagger$	[16]	0.056(0.6)	0.049(6.7)	0.047(9.6)
$\overline{\Lambda}_\Xi/h^-$	$0.042 \pm 0.004^\dagger$	[16]	0.042(0.0)	0.036(2.0)	0.035(2.8)
Λ_Ξ/p	0.90 ± 0.12	[10]	0.805(0.6)	0.662(3.9)	0.494(11.5)
$\overline{\Lambda}_\Xi/\bar{p}$	0.93 ± 0.19	[10]	0.899(0.0)	0.730(1.1)	0.543(4.1)
$\pi^\pm/p_\Lambda$	9.5 ± 2	[15]	9.4(0.0)	9.2(0.6)	7.4(27.7)
$\pi^\pm/\bar{p}_\Lambda$	13.4 ± 2.5	[15]	13.7(0.1)	13.3(0.0)	10.6(9.6)
Ξ^-/π	$0.0088 \pm 0.0008^\dagger$	[14]	0.0092(0.2)	0.0097(1.2)	0.0069(5.6)
Ξ^-/h^-	0.0085 ± 0.0015	[14]	0.0076(0.3)	0.0079(0.2)	0.0056(3.8)
$\overline{\Xi^-}/h^-$	0.0070 ± 0.001	[14]	0.0061(0.9)	0.0064(0.4)	0.0046(6.0)
Ξ^-/Λ	0.193 ± 0.009	[14]	0.190(0.1)	0.189(0.2)	0.132(45.4)
$\overline{\Xi^-}/\overline{\Lambda}$	0.221 ± 0.011	[14]	0.207(1.6)	0.206(1.8)	0.144(48.4)
Ω/Ξ^-			0.20	0.21	0.18
$\overline{\Omega}/\overline{\Xi^-}$			0.22	0.23	0.20
Ω/h^-	0.0012 ± 0.0005	[17]	0.0015(0.4)	0.0016(0.7)	0.0010(0.13)
$\overline{\Omega}/\Omega$	0.95 ± 0.1	[17]	0.87(0.7)	0.88(0.5)	0.90(0.3)
ϕ/K^-	0.15 ± 0.03	[18]	0.174(0.6)	0.177(0.8)	0.148(0.0)
ϕ/h^-	0.021 ± 0.001	[18]	0.022(1.2)	0.023(2.5)	0.018(10.2)
T			140.3 ± 1.1	142.5 ± 1.2	165.8 ± 2.2
$\gamma_q^{\rm HG}$			1.64^*	1.63^*	1^*
λ_q			1.070 ± 0.008	1.069 ± 0.008	1.065 ± 0.008
$\mu_{\rm B}$ [MeV]			28.5	28.4	31.3
$\gamma_s^{\rm HG}/\gamma_q^{\rm HG}$			1.50 ± 0.04	1.48 ± 0.04	1^*
λ_s			1.0243^*	1.0218^*	1.0186^*
$\mu_{\rm S}$ [MeV]			6.1	6.4	7.4
E/b [GeV]			34.7	34.3	34.1
s/b			9.48	9.3	7.0
S/b			233.4	227.7	238.5
E/S [MeV]			148.7	150.5	143.0
χ^2/dof			$10/(21-3)$	$25/(21-3)$	$188.2/(21-2)$

The high yields of hyperons require significant (30–40%) corrections for unresolved

weak decays. Some experimental results are already corrected in this fashion: the weak cascading corrections were applied to the most recent p and $\bar{p}$ results by the PHENIX collaboration [10], and in the Ξ/Λ and $\overline{\Xi}/\overline{\Lambda}$ ratio of the STAR collaboration we use here [14]. However, some of the results we consider are not yet corrected [15, 16], and are indicated in the first column in table 1 by a subscript Λ or Ξ. We present two non-equilibrium fits, left with 100% $\Xi \to Y$ cascading acceptance and with 40% $Y \to N$ acceptance. Then, a non-equilibrium fit with 40% $\Xi \to Y$ and 40% $Y \to N$, and in the last column, the chemical equilibrium fit with 40% cascading.

Below the fit results, we show the statistical parameters which are related to each fit, and at the very bottom the χ^2 of the fit. We observe a considerable improvement in the statistical significance of the results of chemical non-equilibrium fits. The results, shown in the table 1, are obtained minimizing in the space of 3 parameters: the chemical freeze-out temperature T, and 2 chemical parameters λ_q, γ_s, the value of γ_q is set at its maximal value, $\gamma_q^2 = e^{m_\pi/T}$, and the value of λ_s is derived from the strangeness conservation constraint. Freeing these parameters does not alter the results, the fit converges to local strangeness neutrality, within a few percent, and to full pion phase space saturation $\gamma_q^2 = e^{m_\pi/T}$.

In the bottom of table 1, we see that the chemical non-equilibrium fit specific strangeness content $s/b \simeq 10$ is 35% greater than the chemical equilibrium result. This originates in $\gamma_s/\gamma_q \simeq 1.5$ (*i.e.,* $\gamma_s \simeq 2.5$). The specific yield of strangeness and strangeness occupancy we measure in the phase space after hadronization is consistent with the expected QGP properties before hadronization with nearly saturated strangeness phase space.

Allowing for chemical non-equilibrium in sudden hadronization, we indeed find a low freeze out temperature $T_h = 140$–$142\,\mathrm{MeV}$. This range of hadronization temperature agrees with supercooling effect for fast expanding QGP [19]. The wind of expanding QGP adds to the thermal pressure, and the combined kinetic and thermal pressure of exploding quark–gluon plasma can press out the confining vacuum cooling below equilibrium hadronization temperature [3, 20].

References

[1] E. Fermi. Prog. Theor. Phys. **5** (1950) 570.

[2] I. Pomeranchuk, Proc. USSR Academy of Sciences **43** (1951) 889.

[3] J. Letessier and J. Rafelski. *Hadrons and Quark-Gluon Plasma*, Cambridge Monogr. Part. Phys. Nucl. Phys. Cosmol. **18** (2002) pp 1–397.

[4] T. Biró and J. Zimányi. *Nucl. Phys.* A, **395,** (1983) 525.

[5] J. Rafelski and B. Müller. *Phys. Rev. Lett.*, **48** (1982) 1066; **56** (1986) 2334E.

[6] B. Combridge. *Nucl. Phys.* B, **151,** (1979) 429.

[7] J. Rafelski and J. Letessier. *Phys. Lett.* B, **469,** (1999) 12.

[8] G. Torrieri and J. Rafelski. New J. Phys., **3** (2001) 12.

[9] W. Broniowski and W. Florkowski. Phys. Rev. Lett, **87** (2001) 27-2302.

[10] C. Adcox, *et al.*, PHENIX collaboration. Phys. Rev. Lett. **89**, (2002) 09-2302.

[11] W. Broniowski, A. Baran, and W. Florkowski. hep-ph/0209286, Acta. Phys. Pol. B (in press 2002).

[12] P. Braun-Munzinger, D. Magestro, K. Redlich and J. Stachel. Phys. Lett. B **41**, (2001) 518.

[13] J. Rafelski, and J. Letessier. hep-ph/0206145 in AIP Conference Proceedings **631** pp. 460-489 (2002); and nucl-th/0209084.

[14] J. Castillo, *et al.*, STAR collaboration. nucl-ex/0210032.

[15] C. Adcox *et al.*, PHENIX collaboration. Phys. Rev. Lett, **88** (2002) 24-2301.

[16] C. Adler *et al.*, STAR collaboration. Phys. Rev. Lett, **89**, (2002) 09-2301.

[17] C. Suire, *et al.*, STAR Collaboration. nucl-ex/0211017.

[18] C. Adler *et al.*, STAR collaboration. Phys. Rev. C **65**, (2002) 04-1901.

[19] J. Rafelski and J. Letessier. Phys. Rev. Lett., **85** (2000) 4695.

[20] T. Csorgo, and J. Zimanyi. nucl-th/0206051.